

Theoretical Examination of O(¹D) Insertion Reactions to Form Methanediol, Methoxymethanol, and Aminomethanol

Brian M. Hays and Susanna L. Widicus Weaver*

Department of Chemistry, Emory University, Atlanta, Georgia 30322, United States

S Supporting Information

ABSTRACT: A computational study of O(¹D) insertion reactions with methanol (CH₃OH), dimethyl ether (CH₃OCH₃), and methyl amine (CH₃NH₂) was performed to guide laboratory investigations of the insertion product molecules methanediol (HOCH₂OH), methoxymethanol (CH₃OCH₂OH), and aminomethanol (HOCH₂NH₂), respectively. The minimum energy and higher energy conformer geometries of the products were determined at the MP2/aug-cc-pVTZ level of theory, and CCSD(T)/aug-cc-pVTZ calculations were performed on the reactants, products, and transition states to examine the insertion reaction energetics. Torsional barriers for internal motion in methanediol, methoxymethanol, and aminomethanol were also determined. It was found that O(¹D) insertion into the C–H bond was the most energetically favored reaction pathway, proceeding through a direct and barrierless insertion mechanism. The pathways of O(¹D) insertion into N–H or O–H bonds are also possible, though these reactions are less energetically favored, as they proceed through an association product intermediate before proceeding to the insertion products. Predictions are presented for the pure rotational spectra for the methanediol, methoxymethanol, and aminomethanol products based on the determined molecular parameters. These results provide an excellent starting point to guide laboratory spectral studies of the products.

■ INTRODUCTION

One of the most enduring scientific mysteries has been the chemical origin of biological systems. A great deal of research in this area focuses on polymer self-assembly and the formation of an RNA world. Yet an understanding of simple chemical mechanisms involving small prebiotic molecular precursors is essential before an understanding of molecular evolution can be achieved. It is here that research in gas-phase physical chemistry, specifically in astrochemistry, has much to offer. The low densities and temperatures of space limit the chemistry that occurs in interstellar environments. Observations show that “terrestrial” chemical complexity only begins to emerge as stars and planets form. Recent astrochemical modeling studies^{1,2} have proposed viable chemical routes that could lead to this terrestrial level of complexity. In this reaction scheme, major components of interstellar ices (water, ammonia, methanol, and formaldehyde) break apart via direct and cosmic-ray induced photolysis to form small radicals. These species become mobile on ice surfaces at temperatures greater than 30 K, and can react through barrierless radical–radical reactions on interstellar grains to produce an array of more complex organic molecules. These ices are then ejected into the gas phase at temperatures greater than 100 K, where subsequent ion–molecule reactions can lead to even greater chemical complexity.

Recent laboratory studies of interstellar ice analogues indirectly show that this type of chemistry may indeed be the main path to complex organic molecules in interstellar environments.³ However, the mechanisms that drive this grain-surface chemistry have not been definitively confirmed through either laboratory or observational studies. Observations of the predicted products of these radical–radical reactions could be used to trace the proposed photolysis-driven

chemistry in interstellar clouds and set quantitative limits to constrain astrochemical models. Of the molecules predicted, the species methanediol (HOCH₂OH), methoxymethanol (CH₃OCH₂OH), and aminomethanol (HOCH₂NH₂) are all formed directly from methanol photolysis products in interstellar ices and are of prebiotic chemical importance. Despite their importance, these molecules have not yet been studied using high resolution spectroscopic methods. This is because laboratory studies of these species are challenging since each of these molecules is difficult to isolate under typical gas-phase terrestrial laboratory conditions.

Methanediol forms readily in aqueous solutions of formaldehyde under terrestrial chemical conditions. The vapor above such mixtures can contain as much as 3% methanediol;⁴ however, a gas-phase spectrum has not been reported. Methanediol is predicted to form in interstellar environments through the reaction between OH and CH₂OH radicals that form from water and methanol photolysis.¹ Previous theoretical studies show that methanediol is stable under typical interstellar cloud conditions,⁵ and is therefore likely to be present in high abundance in interstellar clouds if its predicted formation route is correct.

Similarly to methanediol, methoxymethanol forms terrestrially in aqueous solutions of formaldehyde where methanol has been added as a stabilizer.⁶ In the interstellar medium, methoxymethanol is predicted to form from reactions between CH₂OH and CH₃O in ices.¹ These radicals both form from methanol photolysis within the ice. The detection of

Special Issue: Joel M. Bowman Festschrift

Received: January 22, 2013

Revised: April 16, 2013

methoxymethanol would therefore place quantitative limits on the methanol photodissociation branching ratios under these conditions.²

Aminomethanol forms in terrestrial chemistry in the first step of the reaction between ammonia and formaldehyde, but is highly reactive and goes on to form hexamethylenetetramine.⁷ Hexamethylenetetramine is a major product of industrial chemistry with a large variety of uses ranging from its role in rubber and plastic production to use as an antibiotic.⁴ Theoretical studies show aminomethanol to be stable in the gas phase under typical laboratory and interstellar conditions if subsequent reactions can be quenched.⁸ Aminomethanol is predicted to form from radical–radical reactions between NH_2 and CH_2OH in interstellar ices.¹ These radicals form from the photolysis of ammonia and methanol, respectively. Aminomethanol has been predicted to be the interstellar precursor to glycine, which is thought to form from the gas-phase reaction between protonated aminomethanol and formic acid.⁹ Aminomethanol is therefore a key prebiotic interstellar molecule.

Previous laboratory studies of methanediol, methoxymethanol, and aminomethanol are limited because of the reactivity of these molecules. Methanediol¹⁰ and methoxymethanol¹¹ were studied in matrix isolation experiments using infrared spectroscopy to monitor the products of $\text{O}(^1\text{D})$ reactions with methanol and dimethyl ether, respectively. Methanediol was also formed in a gas-phase experiment investigating the reaction between $\text{O}(^1\text{D})$ and isotopically enriched methanol.¹² Aminomethanol was shown to form during thermal processing of interstellar ice analogues containing water, formaldehyde, and ammonia.¹³

While condensed-phase laboratory studies of these molecules have been conducted, none of these molecules has been studied using the high-resolution gas-phase spectroscopy required to guide astronomical searches. A gas-phase production method must be found before such laboratory studies can be conducted. We aim to further explore $\text{O}(^1\text{D})$ insertion reactions as possible routes to the laboratory production of methanediol, methoxymethanol, and aminomethanol from methanol, dimethyl ether, and methyl amine, respectively. In the proposed experiments, $\text{O}(^1\text{D})$ will react with the stable precursors through an on-the-fly mixing scheme to produce gas-phase target molecules in a supersonic expansion. Pure rotational spectroscopy will then be used to monitor the insertion products. Before such studies can be conducted, spectral predictions and an examination of the insertion reaction energetics are required.

There are previous theoretical studies of the target molecules and their formation through $\text{O}(^1\text{D})$ insertion reactions reported in the literature. The stability and geometry of methanediol was examined by both *ab initio* and density functional theory (DFT) methods by Kent et al.,⁵ while a similar study was conducted for aminomethanol by Feldman et al.⁸ Schalley et al.¹⁴ performed a computational study of the $\text{O}(^1\text{D})$ + dimethyl ether association into dimethyl peroxide using DFT methods. Additionally, Huang et al.¹² performed DFT calculations on the stationary points on the potential energy surface for the $\text{O}(^1\text{D})$ + methanol reaction, used this information to determine the rate coefficients and branching ratios for the various reaction pathways, and experimentally examined $\text{O}(^1\text{D})$ insertion reactions into methanol by observing OH thermal distributions. Despite these previous studies, the full set of information needed to guide laboratory studies of the $\text{O}(^1\text{D})$ insertion reactions and spectroscopic searches for the products is not available. We have therefore conducted high-level calculations

to explore the minimum energy and higher energy conformer geometries and torsional barriers for methanediol, methoxymethanol, and aminomethanol, as well as the energetics of the insertion reactions to form these molecules. Here we report the results of these calculations and the associated spectral predictions based on these results.

CALCULATIONS

All calculations were performed using the Gaussian 09 Quantum Chemistry Package¹⁵ at the Cherry L. Emerson Center for Scientific Computation at Emory University. Each molecule geometry was optimized at the MP2 level of theory^{16–18} using the aug-cc-pVTZ basis set.¹⁹ Although reactions with $\text{O}(^3\text{P})$ can occur in the proposed experiments, it has been shown that abstraction is the dominant pathway for these reactions,²⁰ and triplet insertion products are highly unlikely. Therefore, only the insertion products in the singlet state were examined in this study. Initial guesses were made as to the minimum energy structure for each molecule. The dihedral angles related to the heavy atoms on each molecule were rotated to provide a series of first estimates for possible conformer structures. Each of these structures was then optimized to find a local energy minimum. The global minimum energy structure was then determined through comparison of the energies found for each conformer.

Once the global minimum energy structure was found for each molecule, the energetics of the insertion reaction leading to that product were examined. Calculations were performed along the minimum energy pathway for each insertion reaction, beginning with the starting material (i.e., $\text{O}(^1\text{D})$ + precursor) and ending with the global minimum energy insertion product structure. Some reactions were found to pass through an $\text{O}(^1\text{D})$ association product intermediate along the pathway to the insertion products. The geometries for stationary points found on the potential energy surface were optimized using the MP2/aug-cc-pVTZ level of theory, and single point energies were calculated at the CCSD(T)/aug-cc-pVTZ level of theory.^{16–19,21} The harmonic vibrational frequencies for the optimized structures along the singlet insertion path were found using the MP2/aug-cc-pVTZ level of theory and used to verify transition states.

In addition to exploring the reaction energetics, the resultant molecular parameters for the minimum energy geometry were used to predict spectra at 30 K with Pickett's CALPGM suite of programs²² using a standard asymmetric top Hamiltonian in the Watson-A reduction. The rotational constants and electric dipole moment components used for the spectral predictions were taken from the MP2/aug-cc-pVTZ calculations. The dipole moments components were transformed to the principal axis system before they were included as input parameters for the spectral simulations.

Finally, the torsional barriers were estimated at the MP2/aug-cc-pVTZ level of theory using single point calculations, where the functional groups on each molecule were incrementally rotated and energies were determined for the geometry at each position. The torsional barriers were estimated as the difference between the maximum energy found in each of these calculations and the global energy minimum.

RESULTS AND DISCUSSION

Insertion Reaction Energetics. The stationary points on the potential energy surface for the reactions of the parent molecules with $O(^1D)$ are shown in Figures 1–3. The

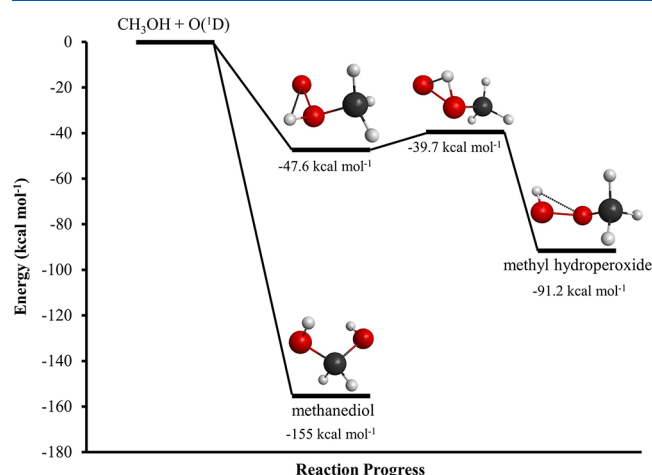


Figure 1. Energies associated with the reaction of $O(^1D)$ and methanol, determined at the CCSD(T)/aug-cc-pVTZ level of theory.

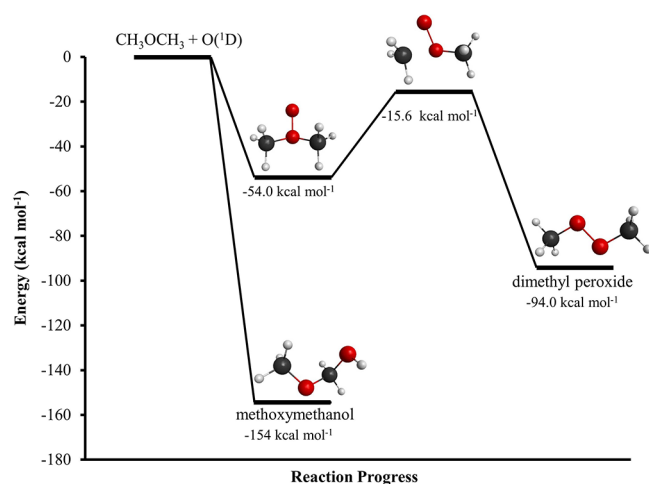


Figure 2. Energies associated with the reaction of $O(^1D)$ and dimethyl ether, determined at the CCSD(T)/aug-cc-pVTZ level of theory.

associated structural information and the vibrational frequencies for those structures are included in the Supporting Information. Each of the $O(^1D)$ insertion reactions was found to be highly exothermic. The $O(^1D)$ insertion reactions into C–H bonds follow a direct and barrierless insertion pathway, while the insertion reactions into N–H or O–H bonds proceed through an association channel before the final product is formed. The $O(^1D)$ insertion reactions into the C–O and C–N bonds were also investigated, despite there being no previous experimental evidence for these insertion products.

In the reaction between $O(^1D)$ and methanol, the formation of methanediol releases 155 kcal/mol of energy, while the formation of methyl hydroperoxide (CH_3OOH) releases 91.2 kcal/mol of energy. In the reaction between dimethyl ether and $O(^1D)$, the formation of methoxymethanol releases 154 kcal/mol of energy, while the formation of dimethyl peroxide (CH_3OOCH_3) releases 94.0 kcal/mol of energy. In the reaction between $O(^1D)$ and methyl amine, several products can form:

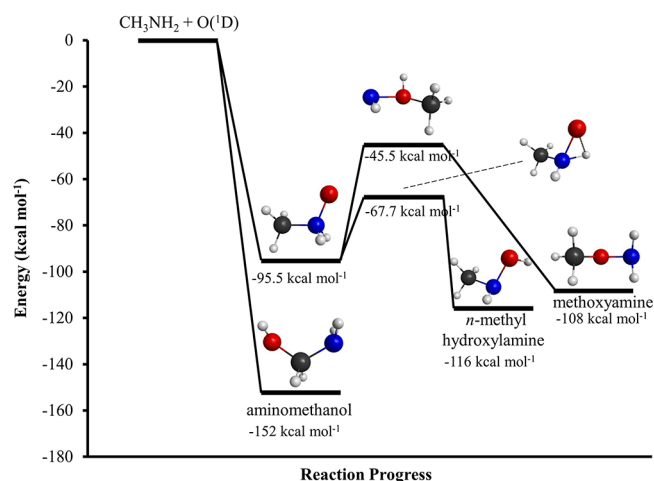


Figure 3. Energies associated with the reaction of $O(^1D)$ and methyl amine, determined at the CCSD(T)/aug-cc-pVTZ level of theory.

aminomethanol forms from $O(^1D)$ insertion into the C–H bond and releases 152 kcal/mol of energy; *n*-methylhydroxylamine (CH_3NHOH) forms from $O(^1D)$ insertion into the N–H bond and releases 116 kcal/mol of energy; and methoxyamine (CH_3ONH_2) forms from $O(^1D)$ insertion into the C–N bond and releases 108 kcal/mol of energy.

The geometries and associated energies determined in this work compare favorably to those reported by Huang et al.¹² for the $O(^1D)$ + methanol reaction. Each of the energies determined for a stationary point in the current work are within 3 kcal/mol of the CCSD(T) results reported in the previous study. In the case of the $O(^1D)$ + dimethyl ether reaction, the geometries determined in the current work agree well with those reported by Schalley et al.,¹⁴ but the energies differ by as much as 10 kcal/mol. However, this previous study used only DFT methods and a smaller basis set. The CCSD(T) energies reported in the current work should therefore be more reliable.

A difference of ~ 20 kcal/mol was noticed between the single point energies determined from the MP2 and CCSD(T) calculations in the current work. Therefore, the multireference nature of these calculations was diagnosed through investigation of the T1 parameter,²³ which was found to range from ~ 0.005 to 0.02 for each of the stationary points in the CCSD(T) calculations. These systems are therefore predominantly single reference in character. Additionally, no spin contamination was suspected because the value of $S(S+1)$ remained at 0 for each calculation. The CCSD(T) calculations were therefore used for the energy comparisons shown in Figures 1–3.

Insertion Product Geometries. The optimized minimum energy geometries for the singlet states of methanediol, methoxymethanol, and aminomethanol are shown in Figure 4, and the corresponding structural information is given in the Supporting Information. The higher-energy conformers for each product are shown in Figure 5, and the corresponding structural information is also given in the Supporting Information. Each of the products is found to have multiple conformers that lie close in energy to the minimum energy geometry. Methanediol has one conformer that is 2.64 kcal/mol higher in energy than the ground state. Methoxymethanol has two conformers that are 2.01 and 2.64 kcal/mol higher in energy than the ground state. Aminomethanol has three

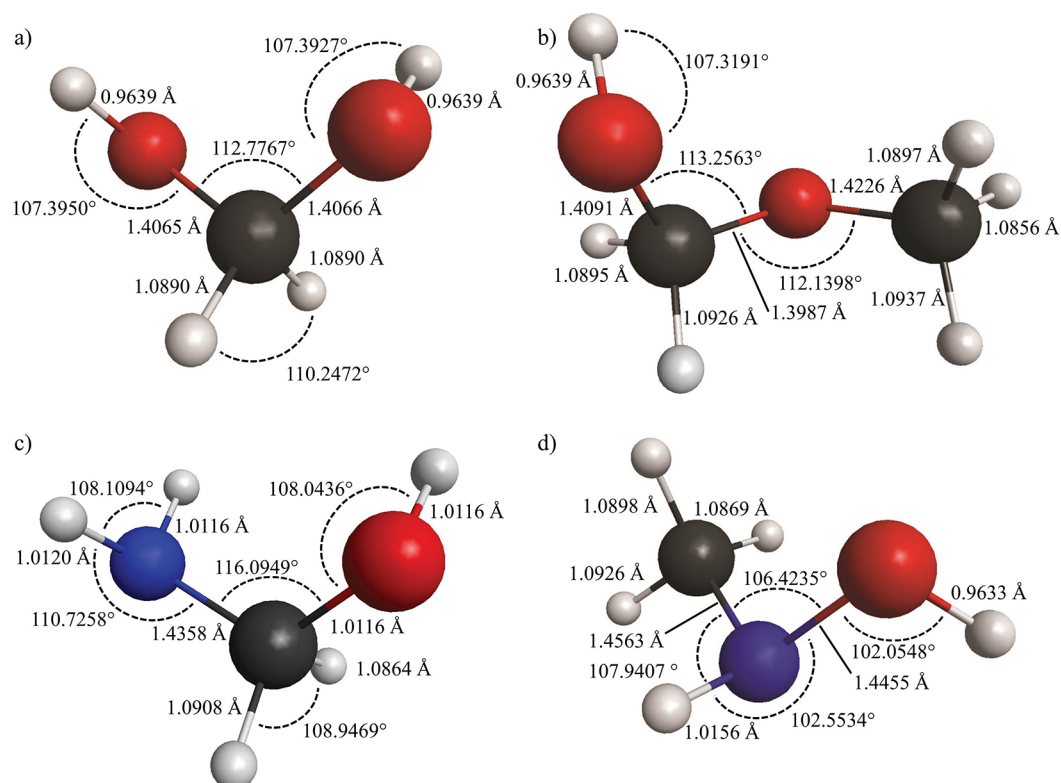


Figure 4. (a) Singlet ground state of methanediol, (b) singlet ground state of methoxymethanol, (c) singlet ground state of aminomethanol, and (d) singlet ground state of *n*-methylhydroxylamine. All structures were optimized at the MP2/aug-cc-pVTZ level of theory.

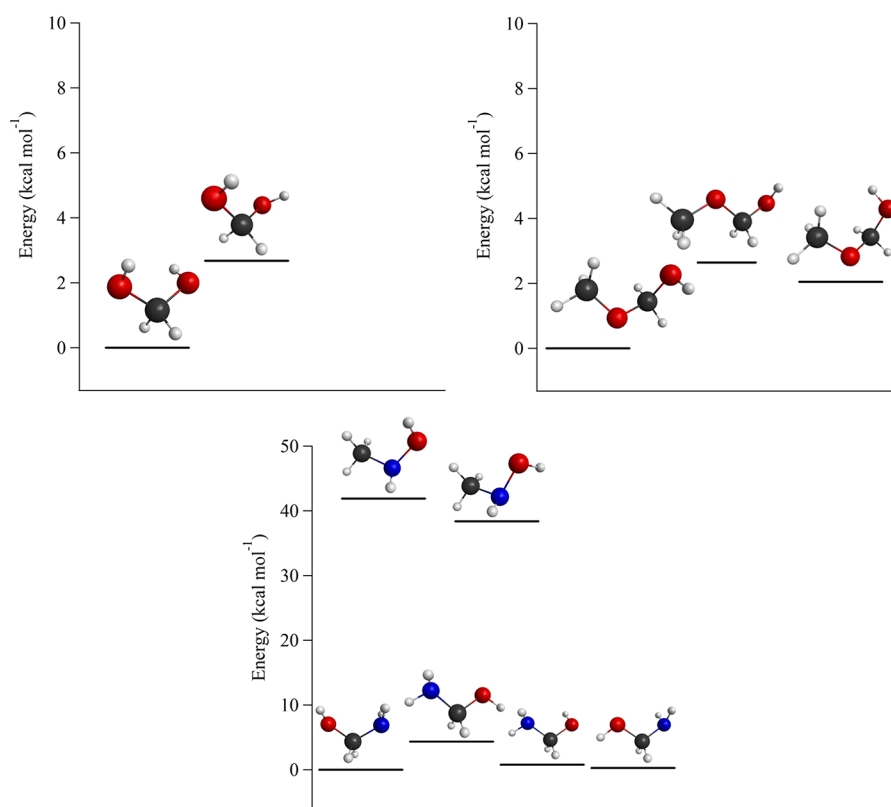


Figure 5. Conformer energies and structures for methanediol (top left), methoxymethanol (top right), and aminomethanol (bottom center). Here the conformer energies are given as relative energies compared to the minimum energy conformer.

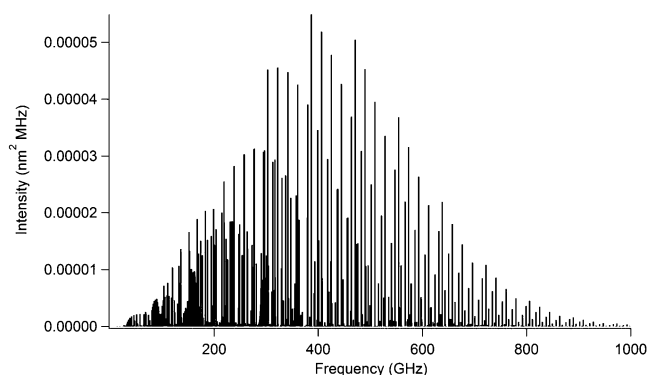
Table 1. Rotational Constants and Electric Dipole Moment Components for the Insertion Products Determined at the at MP2/aug-cc-pVTZ Level of Theory

constant	methanediol	methoxymethanol	aminomethanol	<i>N</i> -methylhydroxylamine
A (GHz)	41.9128	17.1568	38.6930	39.1319
B (GHz)	10.1912	5.6238	9.5457	10.0320
C (GHz)	9.0330	4.8516	8.5868	8.7775
μ_A (D)	0.0089	0.2505	−0.3773	0.6631
μ_B (D)	0.0479	0.0890	−0.9132	−0.4439
μ_C (D)	0.0051	−0.1530	−1.3979	−0.0381

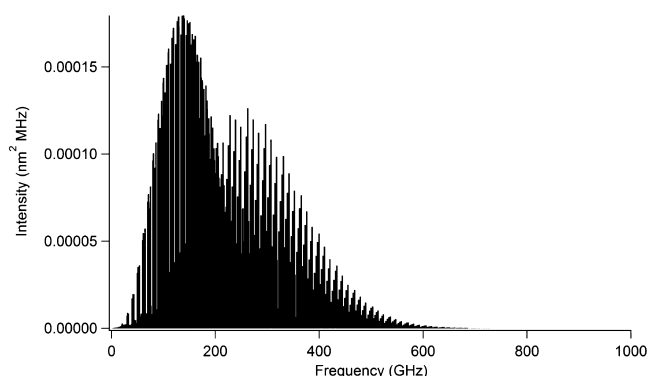
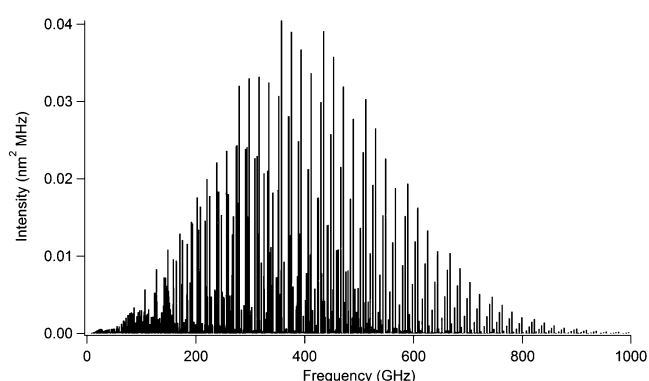
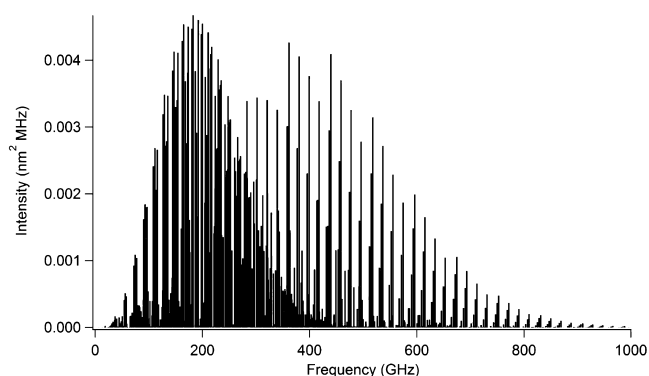
conformers that are 0.30, 0.73, and 4.33 kcal/mol higher in energy than the ground state. The ground state of *n*-methylhydroxylamine is 36.3 kcal/mol above the ground state of aminomethanol, and the next highest energy conformer of *n*-methylhydroxylamine is 39.8 kcal/mol above the ground state of aminomethanol. The reaction of O(¹D) with methanol could also yield methyl hydroperoxide, while the reaction of O(¹D) with dimethyl ether could also yield dimethyl peroxide. Neither of these products was explored in detail in the current work because their structures have already been determined through experiment^{24,25} and theory.²⁶

Spectral Predictions and Barriers to Internal Motion.

The molecular parameters determined from the minimum energy geometries are given in Table 1. Only the rotational constants and components of the electric dipole moment are included, as the centrifugal distortion constants are presumed to be negligible compared to the uncertainties associated with the rotational constants. The information in Table 1 was used to predict the rotational spectrum for each molecule at a temperature of 30 K, which is appropriate for the conditions of the supersonic expansion that will be used for the experimental studies. The resultant spectral predictions generated using Pickett's CALPGM suite of programs²² and assuming a standard asymmetric top Hamiltonian in the Watson-A reduction are shown in Figures 6–9.

**Figure 6.** Prediction of the pure rotational spectrum of methanediol at $T = 30$ K.

An important consideration in the spectral study of small organic molecules is the potential for internal motion in the molecule, which can significantly complicate the spectrum. Therefore, the torsional barriers to internal motion of the functional groups for each product molecule were estimated by incrementally rotating the dihedral bond angles and performing single-point calculations at each step. The torsional potential energy surfaces determined from these calculations are presented in the Supporting Information. From these calculations, the hydroxyl wagging in methanediol was found

**Figure 7.** Prediction of the pure rotational spectrum of methoxymethanol at $T = 30$ K.**Figure 8.** Prediction of the pure rotational spectrum of aminomethanol at $T = 30$ K.**Figure 9.** Prediction of the pure rotational spectrum of *n*-methylhydroxylamine at $T = 30$ K.

to have a barrier of ~ 1689 cm^{−1}. This is a reasonably high barrier, and spectral splitting resulting from this motion is expected to be minimal. For methoxymethanol, both the rotation of the methyl group and the wagging of the hydroxyl

group were examined. The hydroxyl wag was found to have a barrier of $\sim 1697\text{ cm}^{-1}$, which is again sufficiently high to result in negligible spectral splitting. However, the barrier to methyl rotation was found to be $\sim 669\text{ cm}^{-1}$, which indicates that the methoxymethanol spectrum will display standard methyl rotor internal rotation splitting. In the case of aminomethanol, the wagging motions of the amine group and the hydroxyl group were examined. The barrier for the amine wag was found to be 2140 cm^{-1} , which is sufficiently high to preclude torsional spectral splitting. However, the barrier for the hydroxyl wag was found to be 684 cm^{-1} , which will result in torsional spectral splitting. The other molecule that might form from the reaction of methyl amine with $\text{O}(^1\text{D})$ is *n*-methylhydroxylamine. The barrier to methyl rotation is $\sim 1384\text{ cm}^{-1}$ for this molecule, while the barrier for wagging of the hydroxyl rotor is $\sim 2405\text{ cm}^{-1}$; no torsional splitting is expected to be observed in the resultant spectrum. The effects of internal motion for methoxymethanol and aminomethanol were not included in the spectral simulations shown in Figures 7 and 8, but are likely to be important factors in the spectral analyses for these molecules.

Of the molecules studied in this work, only *n*-methylhydroxylamine has experimentally measured spectral information to which a comparison can be made. A low-frequency rotational spectroscopic study of *n*-methylhydroxylamine has been reported.²⁷ The rotational constants determined in the present work agree with that study to within 200 MHz, which is well within the expected uncertainties based on the geometry optimizations presented here. Additionally, the experimentally determined barrier to methyl rotation in *n*-methylhydroxylamine is reported to be $\sim 120\text{ cm}^{-1}$ lower than what was found in the torsional barrier analysis presented above. Again, this is well within the expected uncertainties associated with the calculations.

CONCLUSION

Here we present the results of the most complete computational study to date of $\text{O}(^1\text{D})$ insertion reactions with methanol, dimethyl ether, and methyl amine. We conducted high-level calculations to explore the minimum energy and higher energy conformer geometries and torsional barriers for methanediol, methoxymethanol, and aminomethanol, as well as the energetics of the insertion reactions. It was found that $\text{O}(^1\text{D})$ insertion into the C–H bond was the most energetically favored pathway, proceeding through a direct and barrierless insertion mechanism. The pathways of $\text{O}(^1\text{D})$ insertion into N–H or O–H bonds are also possible, though these reactions are less energetically favored because they proceed through an association product intermediate before proceeding to the insertion products. These results indicate that a laboratory study using a supersonic expansion source for the reaction of $\text{O}(^1\text{D})$ with methanol, dimethyl ether, or methyl amine will favor the C–H bond insertion product as the dominant product of the reaction.

Spectral simulations were generated for the dominant insertion products based on the results of the geometry optimizations. Torsional splitting is expected to be observed in the spectra of methoxymethanol and aminomethanol, but the splitting was not included in the spectral simulations. These results provide an excellent starting point to guide laboratory spectral studies of the products.

ASSOCIATED CONTENT

Supporting Information

The structural information and vibrational frequencies for the stationary points on the singlet surfaces; torsional potential energy surfaces. This material is available free of charge via the Internet at <http://pubs.acs.org>.

AUTHOR INFORMATION

Corresponding Author

*E-mail: susanna.widicus.weaver@emory.edu.

Notes

The authors declare no competing financial interest.

ACKNOWLEDGMENTS

The authors thank Michael Heaven for providing useful guidance about the CCSD(T) calculations, Thomas Anderson for performing preliminary calculations, and John Mancini for providing guidance regarding conversion of the dipole moment components to the primary axis system. The authors also thank Emory University for the facilities and staff support that enabled this work. This work was funded in part by NASA award NNX11AI07G. The authors also acknowledge NSF MRI-R2 grant (CHE-0958205) and the use of the resources of the Cherry Emerson Center for Scientific Computation. All other support came from SLWW's startup funds provided by Emory University.

REFERENCES

- (1) Garrod, R. T.; Widicus Weaver, S. L.; Herbst, E. Complex Chemistry in Star-Forming Regions: An Expanded Gas-Grain Warm-Up Chemical Model. *Astrophys. J.* **2008**, *682*, 283–302.
- (2) Laas, J. C.; Garrod, R. T.; Herbst, E.; Widicus Weaver, S. L. Contributions from Grain Surface and Gas Phase Chemistry to the Formation of Methyl Formate and its Structural Isomers. *Astrophys. J.* **2011**, *728*, 71 (9pp).
- (3) Öberg, K. I.; Garrod, R. T.; van Dishoeck, E. F.; Linnartz, H. Formation Rates of Complex Organics in UV Irradiated CH_3OH -Rich Ices. *Astron. Astrophys.* **2009**, *504*, 891–913.
- (4) Walker, F. J. *Formaldehyde* (Reinhold, New York, 1964)
- (5) Kent, D.R. IV; Widicus Weaver, S. L.; Blake, G. A.; Goddard, W. A., III A Theoretical Study of the Conversion of Gas Phase Methanediol to Formaldehyde. *J. Chem. Phys.* **2003**, *119*, 5117–5120.
- (6) Maiwald, M.; Fischer, H. H.; Ott, M.; Peschla, R.; Kuhnert, C.; Kreiter, C. G.; Maurer, G.; Hasse, H. Quantitative NMR Spectroscopy of Complex Liquid Mixtures: Methods and Results for Chemical Equilibria in Formaldehyde–Water–Methanol at Temperatures up to 383 K. *Ind. Eng. Chem. Res.* **2003**, *42*, 259–266.
- (7) Nielsen, A. T.; Moore, D. W.; Ogan, M. D.; Atkins, R. L. Structure and Chemistry of the Aldehyde Ammonias. 3. Formaldehyde–Ammonia Reaction. 1,3,5-Hexahydrotriazine. *J. Org. Chem.* **1979**, *44*, 1678–1684.
- (8) Feldmann, M. T.; Widicus Weaver, S. L.; Blake, G. A.; Kent, D.R. IV; Goddard, W. A., III. Aminomethanol Water Elimination: Theoretical Examination. *J. Chem. Phys.* **2005**, *123*, 034304–1–6.
- (9) Charnley, S. Interstellar Organic Chemistry. In *The Bridge Between the Big Bang and Biology*, Giovanelli, F., Ed.; Consiglio Nazionale delle Ricerche: Rome, 2001; p 139.
- (10) Lugez, C.; Schriver, A.; Levant, A.; Schriver-Mazzuoli, L. A Matrix-Isolation Infrared Spectroscopic Study of the Reactions of Methane and Methanol with Ozone. *Chem. Phys.* **1994**, *181*, 129–146.
- (11) Wrobel, R.; Sander, W.; Kraka, E.; Cremer, D. Reactions of Dimethyl Ether with Atomic Oxygen: A Matrix Isolation and a Quantum Chemical Study. *J. Phys. Chem. A* **1999**, *103*, 3693–3705.
- (12) Huang, C. K.; Xu, Z.; Nakajima, M. F.; Nguyen, H. M. T.; Lin, M. C.; Tsuchiya, S.; Lee, Y. P. Dynamics of the Reactions of $\text{O}(^1\text{D})$

with CD₃OH and CH₃OD Studied with Time-Resolved Fourier-Transform IR Spectroscopy. *J. Chem. Phys.* **2012**, *137*, 164307.

(13) Bossa, J. B.; Theule, P.; Duvernay, F.; Chiavassa, T. NH₂CH₂OH Thermal Formation In Interstellar Ices Contribution to the 5–8 μ m Region Towards Embedded Protostars. *Astrophys. J.* **2009**, *707*, 1524–1532.

(14) Schalley, C. A.; Harvey, J. N.; Schröder, D.; Schwarz, H. Ether Oxides: A new Class of Stable Ylides? A Theoretical Methanol Oxide and Dimethyl Ether Oxide. *J. Phys. Chem. A* **1992**, *102*, 1021–1035.

(15) Frisch, M. J.; Trucks, G. W.; Schlegel, H. B.; Scuseria, G. E.; Robb, M. A.; Cheeseman, J. R.; Scalmani, G.; Barone, V.; Mennucci, B.; Petersson, G. A.; et al. *Gaussian 09*, revision A.1; Gaussian, Inc.: Wallingford CT, 2009.

(16) Hampel, C.; Werner, H. J. Local Treatment of Electron Correlation in Coupled Cluster Theory. *J. Chem. Phys.* **1996**, *104*, 6286–6297.

(17) Hetzer, G.; Pulay, P.; Werner, H. J. Multipole Approximation of Distant Pair Energies in Local MP2 Calculations. *Chem. Phys. Lett.* **1998**, *290*, 143–149.

(18) Schutz, M.; Hetzer, G.; Werner, H. J. Low-Order Scaling Local Electron Correlation Methods. I. Linear Scaling Local MP2. *J. Chem. Phys.* **1999**, *111*, 5691–5705.

(19) Dunning, T. H. Gaussian Basis Sets for Use in Correlated Molecular Calculations. I. The Atoms Boron through Neon and Hydrogen. *J. Chem. Phys.* **1989**, *90*, 1007–1023.

(20) Gross, R. L.; Liu, X.; Suits, A. G. O(³P) versus O(¹D) Reaction Dynamics with *n*-Pentane: A Crossed Molecular Beam Imaging Study. *Chem. Phys. Lett.* **2003**, *376*, 710–716.

(21) Hampel, C.; Peterson, K.; Werner, H. J. A Comparison of the Efficiency and Accuracy of the Quadratic Configuration Interaction (QCISD), Coupled Cluster (CCSD), and Brueckner Coupled Cluster (BCCD) Methods. *Chem. Phys. Lett.* **1992**, *190*, 1–12.

(22) Pickett, H. M.; Poynter, R. L.; Cohen, E. A.; Delitsky, M. L.; Pearson, J. C.; Muller, H. S. P. Submillimeter, Millimeter, and Microwave Spectral Line Catalog. *J. Quant. Spectrosc. Radiat. Transfer* **1998**, *60*, 883–890.

(23) Scuseria, G. E.; Lee, T. J. Comparison of Coupled Cluster Methods which Include the Effects of Connected Triple Excitations. *J. Chem. Phys.* **1990**, *93*, 5851–5855.

(24) Tyblewski, M.; Ha, T. K.; Meyer, R.; Bauder, A.; Blom, C. E. Microwave and Millimeter-Wave Spectra, Electric Dipole Moment, and Internal Rotation Effects of Methyl Hydroperoxide. *J. Chem. Phys.* **1992**, *97*, 6168–6180.

(25) Haas, B.; Oberhammer, H. Gas-Phase Structure of Dimethyl Peroxide. *J. Am. Chem. Soc.* **1984**, *106*, 6146–6149.

(26) Tonmuphean, S.; Parasuk, V.; Karpfen, A. The Torsional Potential of Dimethyl Peroxide: Still a Difficult Case for Theory. *J. Phys. Chem. A* **2002**, *106*, 438–446.

(27) Sung, E.; Harmony, M. D. Microwave Spectrum, Structure, Quadrupole Coupling Constants, Dipole Moment, and Barrier to Internal Rotation of *N*-Methylhydroxylamine. *J. Mol. Spectrosc.* **1979**, *74*, 228–241.